

Available online at www.sciencedirect.com**SciVerse ScienceDirect**

Energy Procedia 24 (2012) 271 – 280

Energy
Procedia

DeepWind, 19-20 January 2012, Trondheim, Norway

Fatigue analysis of copper conductor for offshore wind turbines by experimental and FE method

Fachri P. Nasution¹,*Department of Marine Technology, NTNU, Otto Nielsens vei 10, 7491, Trondheim*

Svein Sævik

Department of Marine Technology, NTNU, Otto Nielsens vei 10, 7491, Trondheim

Janne.K.Ø. Gjøsteen

Norwegian Marine Technology Research Institute, MARINTEK, Otto Nielsens vei 10, 7052, Trondheim

Abstract

The objective of this work was to investigate the fatigue performance of a 95 mm² copper conductor. The compacting procedure applied during the manufacturing process causes geometrical irregularities in the wires. Specimens from different layers have been tested in tension-tension mode with a stress-ratio, $R = 0.1$. The irregularities have been measured and through numerical studies applied to assess the resulting bending stresses in tension loading. When this is accounted for, the fatigue behavior of the core and the outer layer seems to be similar. This indicates that the difference in fatigue data observed between different layers of wires can be explained by surface irregularities. However, this needs to be supported by more data.

© 2012 Published by Elsevier Ltd. Selection and/or peer-review under responsibility of SINTEF Energi AS.
Open access under [CC BY-NC-ND license](http://creativecommons.org/licenses/by-nc-nd/4.0/).

Keywords: Fatigue analysis, stress range levels, copper conductor, irregularities, stress ratio.

1. Introduction

Power cables have a wide range of applications both onshore and offshore. They are extensively used in electromechanical and communications links, power transmission lines and also electrification of floating production systems of oil and gas. Another application area is transmission lines for floating offshore wind turbines. In such a case fatigue may become a limiting factor due to the dynamic nature of the system. The critical section with respect to dynamic loads will in most cases be the top connection region (see Fig.1).

The power cables may consist of multiple conductors, where each conductor represents an assembly of individual wires which are usually made of copper or aluminium. See Fig. 2a for a typical offshore power

^{☆1} Corresponding author Tel: +47 735 955 64

Email address: fachri.nasution@ntnu.no (Fachri P. Nasution)

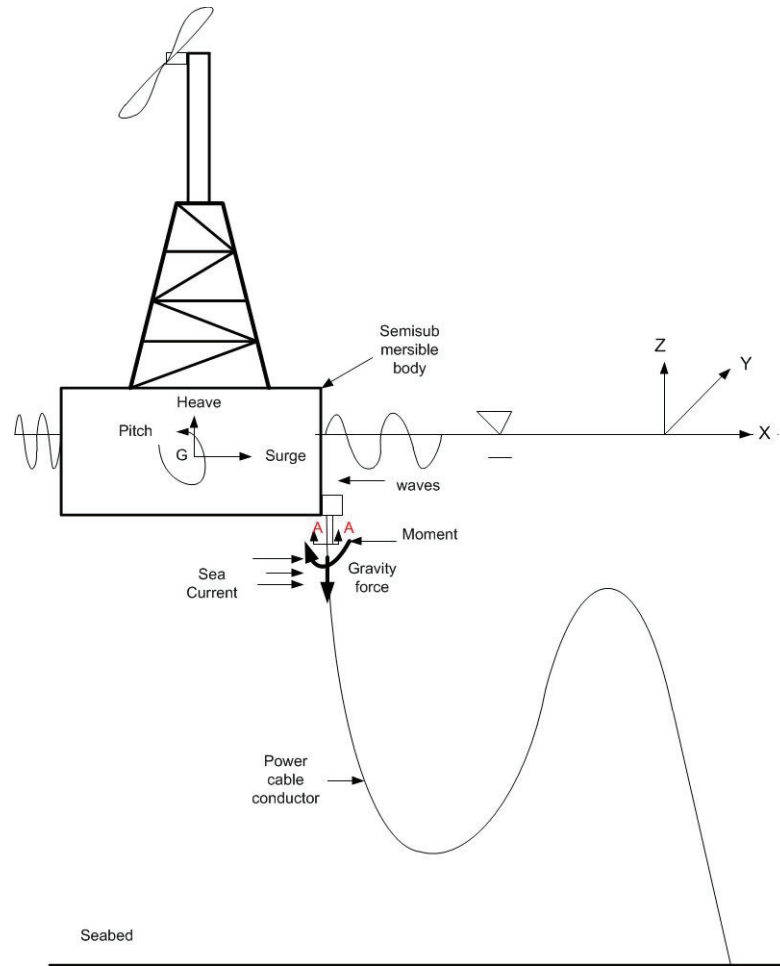


Fig. 1. Power cable conductor attached on floating offshore wind turbine

cable for an AC (Alternating Current) system. This cable is composed of three phases of helically stranded copper conductors. Each conductor consists of copper wires wrapped in layers around a centre wire.

During operation, the cable will be exposed to both static and dynamic loading. The gravity will induce a mean global tension (\bar{T}) and a mean global torque moment (\bar{M}_T), see Fig. 2a. The wave and current loads are of dynamic nature, and will induce transverse hydrodynamic loads on the cable. This will cause variations in tension (ΔT) torque (ΔM_T) and curvature ($\Delta\beta$) along the cable.

Mean and dynamic tension will be transferred to the individual wires primarily as tension forces while the dynamic bending moment will induce local bending as well as axial friction forces in each individual wire. The static load condition in each wire is governed by the mean axial force (\bar{F}_x), which again is governed by the mean global tension (\bar{T}) and the mean global torsion moment (\bar{M}_T). See Fig. 2b. The dynamic axial force (ΔF_x) in each wire is a function of the mean axial force and the corresponding dynamic quantities ΔT and ΔM_T , the dynamic curvature ($\Delta\beta$), and the coefficient of friction (μ) between the contact surfaces. The dynamic curvature results in local bending in each wire, where ΔM_x , ΔM_y and ΔM_z are the dynamic torque moment about the helix tangential x-direction, dynamic bending moment about the helix bi-normal y-direction and dynamic bending moment about the surface normal z-direction, respectively. Due to the dynamic tension and bending of the wires, the fatigue strength becomes an important design issue.

Some investigations dealing with fatigue analysis of spiral strands have been performed, primarily related to wire ropes and cables for structural applications. Hobbs and Ghavami [1] have reported fatigue test results for socketed structural strands. They concluded that several failure mechanisms related to the contact conditions close to the socket govern the fatigue behavior. Raof [3] developed from first principles a theoretical model using axial single wire data for predicting the axial fatigue of the full cross-section at constant load amplitude, and was able to correlate the theoretical prediction to the observations from experimental testing.

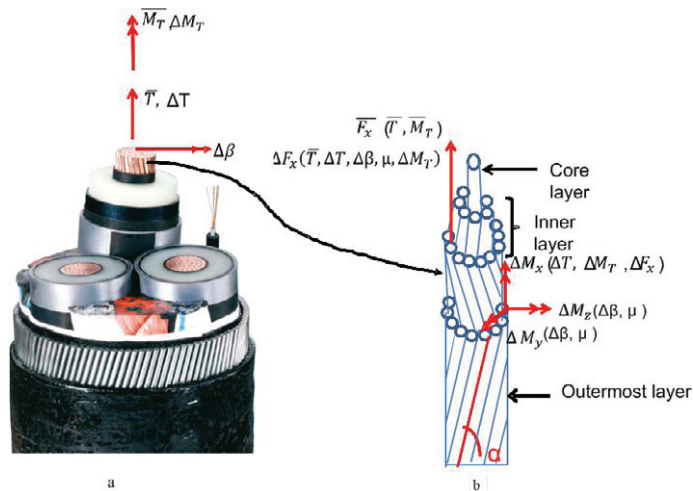


Fig. 2. a. Offshore power cable with three phases for AC system using helically stranded copper conductor inside (at section A-A in Fig. 1[2]). b. Helically stranded copper conductor with lay angle α exposed to dynamic and static loadings.

Casey and Lee [4] described the degradation of large diameter six strands wire ropes when subjected to constant amplitude tension-tension fatigue. Raof [5] concluded that his theoretical model provides useful upper bounds to the fatigue life of cables failing at the end termination and that the termination type significantly affects the observed fatigue life. He also showed that using sheathed spiral strands in deep waters theoretically will exhibit reductions in the axial fatigue life. Raof and Davies [6] extended the previously developed axial fatigue model by carrying out parametric studies on large diameter sheathed spiral strand constructions, covering a huge range of manufacturing lay angles α . They also constructed S-N curves for sheathed spiral strands for deep water structural applications based on the obtained model and test data.

As opposed to the aforementioned authors, the present study focus on copper conductors applied in dynamic cables where the design is based on using protective steel armours and bending stiffeners to resist the external forces, thus limiting the tensile forces and curvatures in the stranded copper conductor. The configuration of the dynamic cable is designed to limit the dynamic tension. Hence the load condition for the dynamic power conductor will be significantly different, governed by moderate average tension, small dynamic tension variations and moderate dynamic curvatures. Normal design practice for such applications has been to limit the allowable tensile strain to 0.10-0.15 %.

Karlsen [7] performed fatigue testing of individual wires as well as 28 full cross-section power conductors in rotation bending. The bending tests were carried out at constant tension and variable curvature representative for deep water applications. However, no details were given with regard to the failures. Nasution, Sævik and Gjøsteen [8] also performed axial fatigue testing of individual wires for copper conductor and presented an S-N curve. The results were in the same range as those presented by Karlsen.

The present paper focus on investigations related to the correlation between the location of failures seen in fatigue testing versus observed surface irregularities and stress ranges obtained by finite element (FE) analysis. This is done in order to provide better understanding of the fatigue performance of individual wires thus enabling more rational selection of specimens for characterizing the fatigue life of conductor cross-sections.

A 95 mm² copper conductor was investigated. One application area for this type of structure is floating offshore wind turbines. The conductor is a stranded structure, and due to the compacting procedure applied during the manufacturing process geometrical irregularities were observed in the wires. The irregularities were largest in the outer layer. Specimens were therefore taken from both the centre and the outer layer to assess the difference in fatigue behavior within the cross section. The single wire specimens were tested in tension-tension mode with a stress-ratio, $R = 0.1$. The surface irregularities were measured and used as a basis for correlation analysis with respect to the fatigue failure locations. FE analyzes were then conducted to quantify the bending stresses in pure tension loading.

2. Specimens and Equipment

The specimens used in this work were taken from a 95 mm² copper conductor (ETP copper), designated by the UNS C11000 series. The definition of ETP copper is related to copper alloy purity of at least 99.95% and characterized by a very high electrical conductivity and ductility. The conductor cross section consisted of 19 wires, each with a diameter of 2.5 mm. A centre wire is followed by six and twelve helically wound wires in two layers. The pitch lengths were measured to be 220 mm for both layers. When using the right hand lay rule the obtained lay angles were -4.1° and $+7.3^\circ$ for the inner and outer layers, respectively. See Fig. 3a. The manufacturing procedure in this case included compacting the cross-section to a reduced diameter, resulting in observed surface irregularities for the helix layers. Due to the opposite lay angles of the helical layers, the surface irregularities were found to be periodic with a wavelength of approx. 20 mm, see Fig. 4. When applying axial tension, this will result in a bending moment on the wire. The corresponding bending stresses were estimated by FE analysis based on the measured irregularities. The applied copper material properties were based on the measured strain-stress curve of a straightened outer layer wire specimen. Specimens were taken from both the centre wire and the helical layers to investigate possible differences in the fatigue performance and if these differences can be explained by the observed imperfections. The specimens were cut, straightened and terminated at the ends using tubular aluminium tubes filled by standard high strength glue, see Fig. 3b.

The surface irregularities were found to be most significant for the outer layer, characterized by a mean thickness reduction amplitude of 0.44 mm with a coefficient of variation of (COV) of 0.063. The obtained strain-stress curve of the straightened outer layer specimen is shown in Fig. 5. The copper yield strength is commonly defined as the stress resulting in 0.2 % residual strain, which is found to be approximately $\sigma_y = 250$ MPa. The proportional limit is defined as the highest stress at which the material still behaves elastic, in this case taken to be $\sigma_{prop} = 150$ MPa.

The fatigue specimens were tested in constant amplitude axial tension corresponding to nominal stress ranges of ($\Delta\sigma$): 130, 160, 190 and 220 MPa. The nominal stress range is based on a 5 mm² area. The

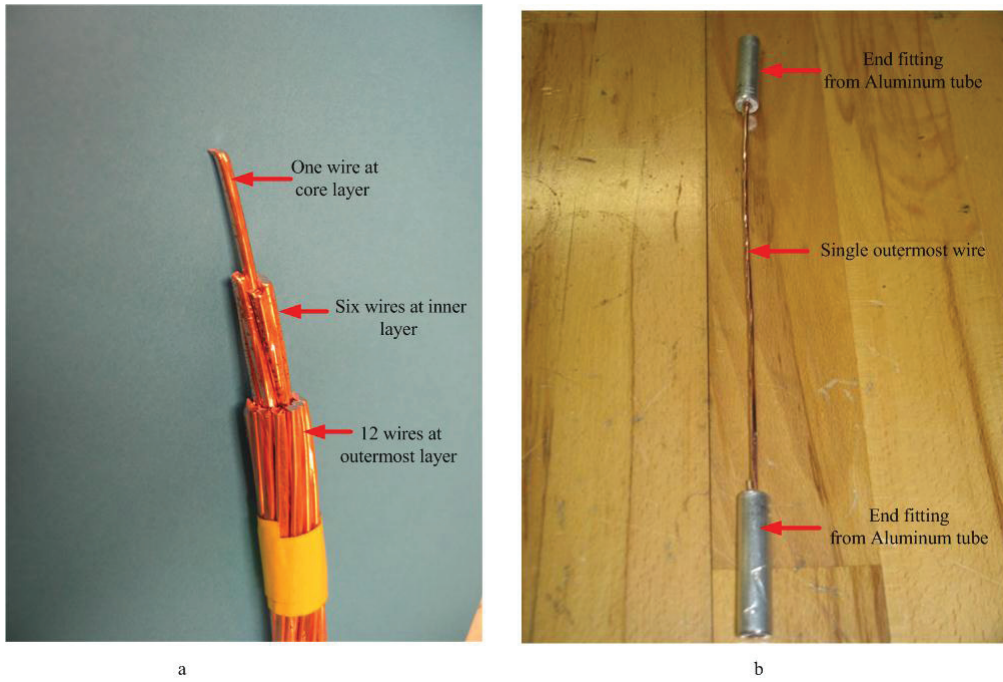


Fig. 3. a) Full cross section of stranded copper conductor; b) an individual outer wire with aluminium tubes at both ends

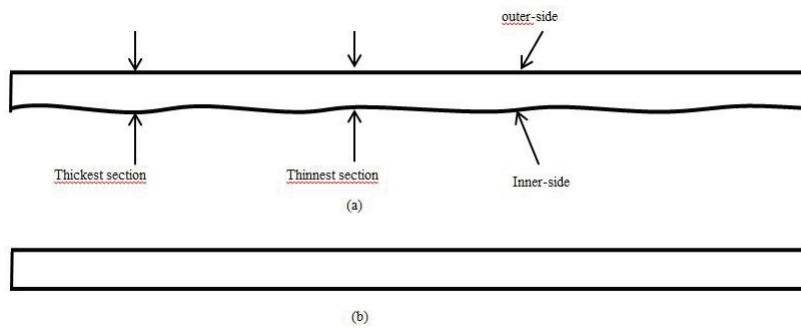


Fig. 4. a. Geometrical surface of outer wire including irregularities; b) Geometrical surface of smooth centre wire

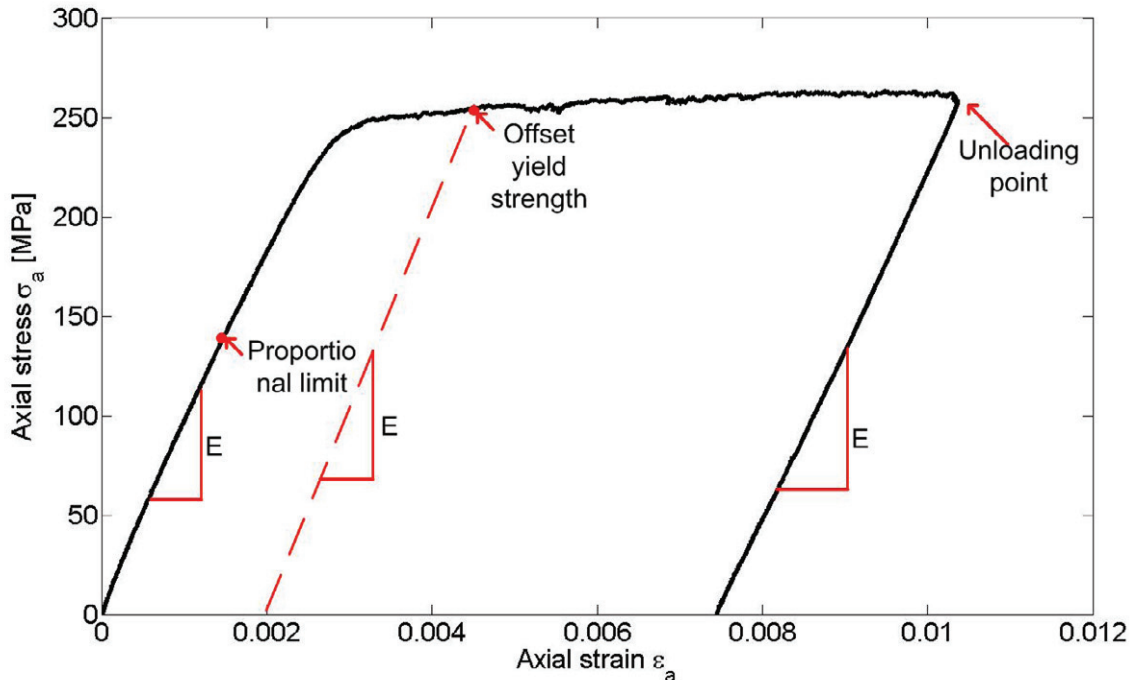


Fig. 5. Strain-stress curve of outer wire

loading test frequency, f , was 2 Hz harmonic loading (sinusoidal) with R-ratio, $R = 0.1$. The cyclic axial load was applied using a standard fatigue testing machine. The specimens were clamped in both ends. see Fig. 6.

3. FE-model

A finite element model was made in order to investigate the effects from measured thickness irregularities and material plasticity with respect to the expected stress range at the material surface. This was performed by applying a 100 mm long elastoplastic beam model, using the measured strain-stress curve, a kinematic hardening model and element eccentricities according to the average measured thickness irregularity. The computer code Uflex3d was applied, using 48 integration points in the cross-section. The dynamic tension-tension fatigue load history was applied according to the fatigue test program and throughout six cycles to eliminate transient effects from material plasticity. An illustration of the detailed FE-model is presented in Fig. 7.

Let us consider the axial stress range, $\Delta\sigma = 190$ MPa. Based on the strain-stress curve in Fig. 5, the applied stress range is larger than proportional stress (σ_{prop}) but still below its yield stress. In addition, the combined action of eccentricity and axial force induces an increase of the tensile stresses at the lower side in Fig. 7 and a reduction at the upper side. The neutral axis will shift position, thus modifying the stress range for the steady state condition. The resulting strain stress-curve at the outer fiber is shown Fig. 8. The resulting stress range in steady state condition is found to be 244 MPa for the 190 MPa nominal stress range case. Thus significant reduction in fatigue capacity is expected for the outer layer wires compared to the smooth centre wire. It is also to be expected that the fatigue failures should occur at the thinnest sections.

For the 130, 160 and 220 MPa nominal stress ranges, the numerical results for the outer layer wire including the bending stresses were 174, 211 and 261 MPa, respectively.



Fig. 6. Detailed on both ends of specimen are clamped against the rotation

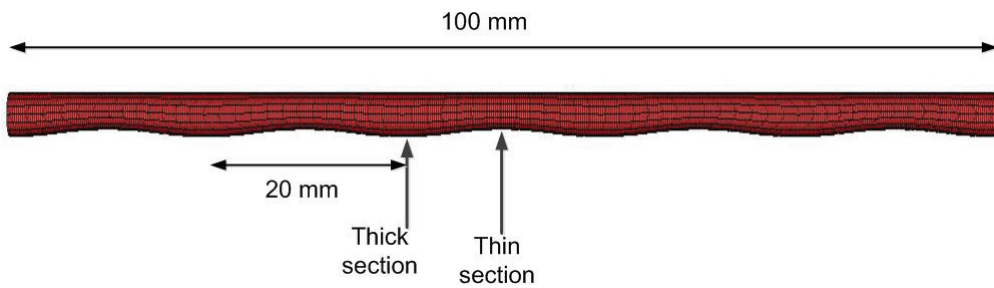


Fig. 7. FE-model of outer wire including irregularities.

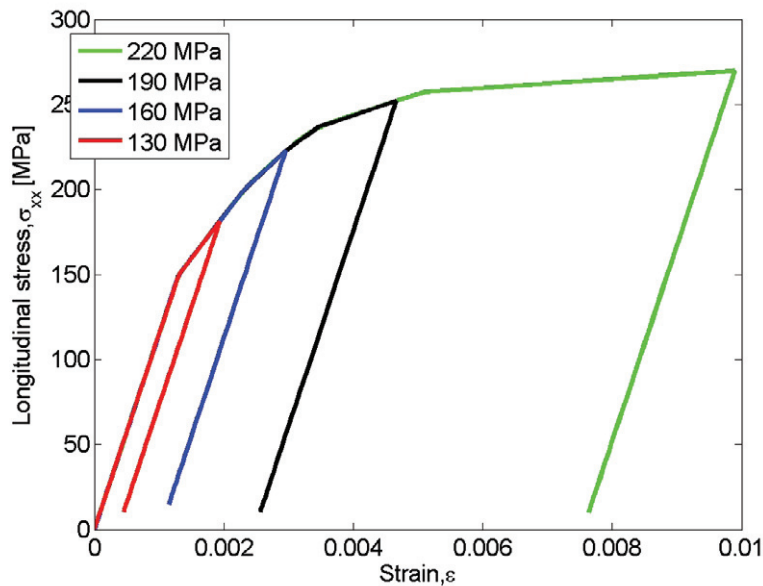


Fig. 8. Strain-stress result of outer wire with R-ratio = 0.1 and $\Delta\sigma = 190$ MPa

4. Results and Discussion

A total of 26 single wire fatigue tests have been carried out per date. 23 of the specimens were taken from the irregular outer layer wires whereas 3 specimens were taken from the smooth centre wire. For the outer layer 13 failures occurred at the mid span while the remaining failed at the end fitting. All midspan failures occurred at the thinnest cross-section in accordance with the FE model prediction. The mid span data has been applied to construct a S-N curve based on the formulation:

$$N(\Delta\sigma)^m = A, \quad (1)$$

where N denotes the number of cycles to failure, m is a constant for the slope, $\Delta\sigma$ is the applied stress range and A is a constant. The scattered fatigue test data are approximated using regression linear analysis by MATLAB in order to find the S-N curve parameters. The resulting values using the nominal stress (no bending correction) were: $m = 6.238$ and $A = 6.098 \cdot 10^{19}$.

Fig. 9 shows the experimental data and the S-N curve obtained for the outer layer wires based on nominal stress ranges, and two curves representing the one standard deviation scatter band. It also includes a S-N curve based on the outer layer wire data, but accounting for stress ranges including bending instead of using the nominal values.

For the centre wires no significant irregularities were observed, meaning that the nominal stress values give a good representation of the stress levels. The test results for all 3 specimens are included in Fig. 9. It is to be noted however that two of the tests failed at the end fitting.

The only valid centre specimen test failed at 1.14×10^6 cycles. This point is within the scatter band of the S-N curve which is obtained based in the outer layer, but corrected for bending stresses. It indicates that the difference in fatigue data observed between different layers of wires can be explained by surface irregularities. However, this needs to be supported by more data from fatigue testing and systematic measurements of inherent irregularities.

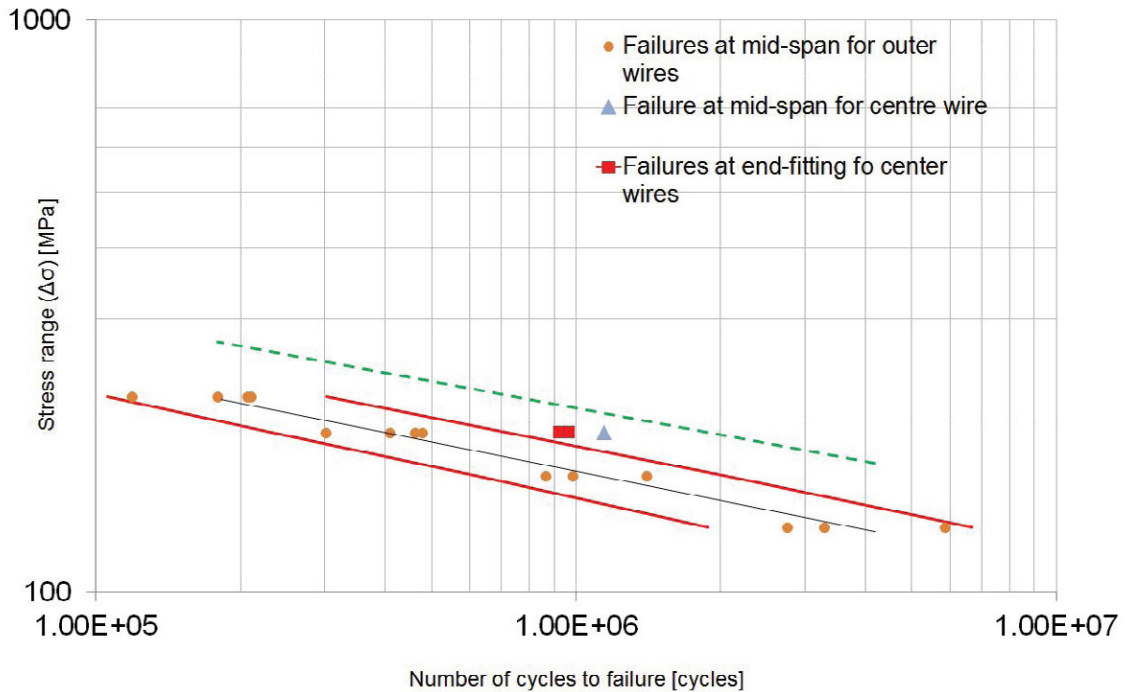


Fig. 9. Fatigue test data. S-N curve of single copper wire for outer layer. The black line shows the S-N curve as obtained based on nominal stress values with the one standard deviation scatter band shown in red lines. The dotted line shows the the S-N curves as obtained for outer layer when including the bending stresses.

5. Conclusions

Fatigue testing of single wire specimens taken from a 95 mm² copper conductor has been carried out. This has been combined with systematic measurements of observed surface irregularities resulting from the manufacturing process and FE analysis to predict their effect on the surface stresses. The results indicates that the differences seen in fatigue performance between layers can be explained by inherent variations in surface irregularities. However, more data are needed in order to conclude on this, both with respect to the copper conductor investigated here and other conductor geometries.

Acknowledgments

We hereby acknowledge ABB for providing the test materials applied in the tests.

References

- [1] Hobbs, R.E and Ghavami, K.. The fatigue of structural wire strands. International Journal of Fatigue 1982; 4:6972.
- [2] Nexans Submarine Technology: Submarine Cables, Umbilicals and Services.
- [3] Raouf, M..Axial Fatigue of multilayered strands. Journal of Engineering Mechanics 1989; 116:20832099.
- [4] Casey, N.F and Lee, W.K. The fatigue failure of large diameter six strand wire rope. International Journal of Fatigue 1989; 11:7884.
- [5] Raouf, M. Axial fatigue life prediction of structural cables from first principles. Proceedings Institution of Civil Engineers 1991; 91: 19-38
- [6] Raouf, M. and Davies, J.T. Axial fatigue design of sheathed spiral strands in deep water applications. International journal of fatigue 2008; 30: 2220-2238.
- [7] Karlson, S. Fatigue of copper conductors for dynamic subsea power cables. Proceedings of the ASME 2010 29th International conference on ocean, offshore and arctic engineering 2010.

- [8] Nasution, F.P., Sævik, S., Gjøsteen, J.K.Ø. Finite element analysis for fatigue prediction of copper conductors applied in offshore wind turbines. Proceedings of IV International conference on computational methods in marine engineering 2011- MARINE 2011.